

Stability Control of Multi-Quadcopter Formation Based on Virtual Leader and Flocking Algorithm

Nilla Perdana Agustina¹, Purwadi Agus Darwito^{2*}, Bambang L. Widjiantoro³, Murry Raditya⁴

^{1,2,3} Department of Engineering Physics, Sepuluh Nopember Institute of Technology, Surabaya, Indonesia

⁴ Department of Civil and Construction Engineering, National Taiwan University of Science and Technology, Taipei, Taiwan
Email: ¹7009231002@student.its.ac.id, ²padarwito@ep.its.ac.id, ³blelono@ep.its.ac.id, ⁴D11305817@mail.ntust.edu.tw

*Corresponding Author

Abstract—This study aims to develop an efficient and stable formation strategy for multi-quadcopter systems, focusing on formation stability based on the number of flying quadcopter members. The formation strategy combines a virtual leader approach and flocking-based behavior to achieve consistent formation movement. The formations are designed as basic circular and elliptical patterns based on bearing measurement. Formation control in multi-quadcopter systems presents a complex challenge, as it requires coordination among autonomously flying UAVs while maintaining overall formation stability and reliability. A Twisted Sliding Mode Control (TSMC) system is implemented to ensure formation stability and responsiveness to predefined trajectory missions. After integrating TSMC, the Root Mean Square Error (RMSE) of position errors in the x, y, and z coordinates decreased by 0.02.

Keywords—Multi Quadcopter; Virtual Leader; Algorithm Flocking; Twisted Sliding Mode Control.

I. INTRODUCTION

The use of unmanned aerial vehicles (UAVs) has increased significantly across various applications. [1][2], including surveillance, search and rescue [3]–[5], and military operations [6]–[9]. While offering numerous advantages, individual UAVs face limitations in area coverage, operational efficiency, and coordination capabilities with other units [10]–[12]. These constraints reduce UAV effectiveness in missions requiring large-area surveillance or search operations [13][14]. Consequently, new strategies are needed to address these challenges, one of which involves multi-UAV systems. Multi-UAV systems provide solutions to overcome individual UAV limitations through inter-UAV cooperation [15]–[17]. Key advantages include expanded coverage area, enhanced operational efficiency, and improved resilience against external disturbances through redundancy and coordination [18]–[20]. Thus, multi-UAV systems have become an important research focus for improving operational effectiveness across various application domains [21]–[23].

Research on multi-UAV formations focuses on formation control [24][25], formation reconfiguration [26]–[28], real-time path planning [29]–[31], etc. Formation control serves as the foundation and primary focus of flight formations [32]. Key aspects of formation control include formation strategy design, communication [33][34], and control systems [35]. Several approaches have been proposed, such as leader-follower methods [36]–[39], virtual structure-based approaches [40][41], behavior-based methods [42]–[44],

consensus-based algorithms [45][46], and Artificial Potential Field (APF) techniques [47][48]. While these methods have shown promising results, they still present limitations. For instance, leader-follower approaches are vulnerable to single-point failures if the leader UAV encounters problems [49][50], while APF methods often generate suboptimal paths due to local minima issues [51]. Therefore, new strategies are required to overcome these limitations and provide more robust and efficient solutions. This study proposes circular and elliptical formation strategies for multi-quadcopter systems using a virtual leader approach combined with flocking algorithms [52][53]. The strategy is designed to maintain formation stability through Twisting Sliding Mode Control (TSMC), which is expected to improve positional accuracy for each UAV within the formation.

Circular and elliptical formations in multi-UAV systems are recognized as among the most efficient configurations for navigation and coordination [54][55]. Circular formations enable uniform UAV distribution, while elliptical formations are ideal for applications requiring extended monitoring in specific directions, such as border surveillance or elongated terrain mapping [56][57]. However, the primary challenges in multi-UAV formation control involve ensuring stability [58]–[60], precision, and resilience against external disturbances [61]. Sliding Mode Control (SMC) is renowned for its robustness against model uncertainties and external disturbances [62][63]. However, traditional SMC often suffers from chattering issues—high-frequency oscillations that can cause hardware wear and increased energy consumption [64]. To address this, several SMC variants have been developed, including Twisting SMC [65][66], Super Twisting Observer SMC [67][68], and Stochastic Event-Based Super-Twisting [69].

This study proposes circular and elliptical formation strategies for multi-quadcopter systems utilizing a virtual leader approach combined with flocking algorithms. The strategy is designed to maintain formation stability through Twisting Sliding Mode Control (TSMC), which is expected to enhance the positional accuracy of each UAV within the formation. Furthermore, this research will explore practical implications of the proposed strategy, including potential applications in wide-area surveillance, mapping, and search-and-rescue operations. By introducing this novel strategy, the study aims to make significant contributions to developing more effective and robust multi-UAV systems. The outcomes are expected to not only enrich the literature on multi-UAV



formation control but also provide practical solutions to enhance multi-UAV system performance in various real-world applications.

The proposed virtual leader strategy addresses limitations of traditional leader-follower approaches, which are vulnerable to single-point failures when the lead UAV encounters issues [70]. By employing a virtual leader, the system eliminates dependence on any specific physical UAV, thereby improving formation resilience and flexibility [71][72]. Additionally, the flocking algorithm ensures effective inter-UAV coordination, even in dynamic and obstacle-rich environments [73]. Previous studies implementing virtual leader-flocking combinations demonstrated successful obstacle avoidance and regrouping near target virtual leaders [74]. However, the accuracy of each agent's position was not further analyzed in the study. The combination of these two approaches is expected to result in stable and accurate formations. The TSMC implementation as the primary control system is also expected to mitigate chattering issues prevalent in conventional SMC [75]. Thus, this strategy offers a more comprehensive solution to the challenge of formation formation on multi-UAV systems.

The practical implications of this research include applications in a variety of fields, such as wide area surveillance, mapping, and search and rescue operations. For instance, elliptical formations prove optimal for monitoring border areas or elongated territories, while circular formations excel in confined-area search operations [76]. The proposed strategy is further adaptable to environmental monitoring, precision agriculture, and logistics applications. Thus, this study provides both theoretical contributions to formation control algorithms and demonstrates wide-ranging real-world applicability. The findings are expected to establish a foundation for developing more advanced and effective multi-UAV systems in future research.

II. METHOD

A. Multi Quadcopter

This study considers a multi-quadcopter system consisting of n agents, where $n \geq 2$. The interactions between quadcopter agents are expressed according to Equation (1).

$$G = (V, E) \quad (1)$$

where $V = \{v_1, v_2, \dots, v_n\}$ represents the set of agents in the formation or collection of nodes and $E = \{e_{ij} | v_i, v_j \in V\}$ denotes the set of edges describing the interaction between two agents v_i and v_j [77][78]. Each quadcopter in the formation has a position that can be described in three-dimensional space with coordinates (x, y, z) . The position of each i -th quadcopter at time t is expressed by Equation (2).

$$p_i(t) = [p_{x_i}, p_{y_i}, p_{z_i}]^T \quad (2)$$

is a position vector in \mathbf{R}^3 . Each $p_{x_i}, p_{y_i}, p_{z_i}$ represents the i -th quadcopter's position coordinates along the x, y, z axes respectively [79].

Each quadcopter exhibits translational motion, generating linear position (3).

$$r = [x_i, y_i, z_i]^T \quad (3)$$

This yields the kinematic model equations for each quadcopter (4).

$$\begin{aligned} \dot{x}_i &= (C_{\psi_i} C_{\theta_i})u_i + (C_{\psi_i} S_{\theta_i} S_{\phi_i} - S_{\psi_i} C_{\phi_i})v_i \\ &\quad + (C_{\psi_i} S_{\theta_i} C_{\phi_i} + S_{\psi_i} S_{\phi_i})w_i \\ \dot{y}_i &= (S_{\psi_i} C_{\theta_i})u_i + (S_{\psi_i} S_{\theta_i} S_{\phi_i} + C_{\psi_i} C_{\phi_i})v_i \\ &\quad + (S_{\psi_i} S_{\theta_i} C_{\phi_i} - C_{\psi_i} S_{\phi_i})w_i \\ \dot{z}_i &= (-S_{\theta_i})u_i + (C_{\theta_i} S_{\phi_i})v_i + (C_{\theta_i} C_{\phi_i})w_i \end{aligned} \quad (4)$$

The linear position of each quadcopter i is described by $\dot{x}_i \in \mathbf{R}, \dot{y}_i \in \mathbf{R}, \dot{z}_i \in \mathbf{R}$. The linear position is based on body frame coordinates $v_B = [u_i, v_i, w_i]^T$ [80].

B. Virtual Leader

The virtual leader in the multi-quadcopter system provides consistent guidance and coordination for follower quadcopter agents to achieve the desired formation [81]. The virtual leader's dynamic equations are (5).

$$\begin{aligned} \dot{p}_0(t) &= v_0(t) \\ \dot{v}_0(t) &= u_0(t) \end{aligned} \quad (5)$$

Where, $p_0(t) \in \mathbf{R}^3$ represents the virtual leader position, $v_0(t) \in \mathbf{R}^3$ denotes the virtual leader velocity. The i -th follower quadcopter agent follows Equation (6).

$$\begin{aligned} \dot{p}_i(t) &= v_i(t) \\ \dot{v}_i(t) &= u_i(t) + d_i(t) \end{aligned} \quad (6)$$

with $p_i(t) \in \mathbf{R}^3$ is the i -th follower's position, $v_i(t) \in \mathbf{R}^3$ represents the i -th follower's velocity, $u_i(t)$ is the control input applied to the i -th follower, and $d_i(t)$ denotes the relative position of the i -th follower.

C. Bearing Measurement-Based Formation

Bearing measurement is a technique that utilizes the angle between two agents. Specifically, between a quadcopter agent and the virtual leader. This method allows each quadcopter agent to determine its relative position within the formation without requiring direct distance data [82][83]. The technique employs the horizontal angle (azimuth) θ_i and the vertical angle (elevation) ϕ_i calculated using Equations (7) and (8).

Horizontal Bearing

$$\theta_i = \text{atan2}(y_i - c_y, x_i - c_x) \quad (7)$$

Vertikal Bearing

$$\phi_i = \text{atan}\left(\frac{z_i - c_z}{\sqrt{(x_i - c_x)^2 + (y_i - c_y)^2}}\right) \quad (8)$$

where, x_i, y_i are the x and y coordinates of the i -th quadcopter, and c_x, c_y are the x and y coordinates of the formation center. z_i is the z coordinate of the i -th quadcopter in the vertical plane, c_z is the z coordinate of the formation center. The following illustrates the angular measurement representation in bearing measurement for both 2D and 3D spaces.

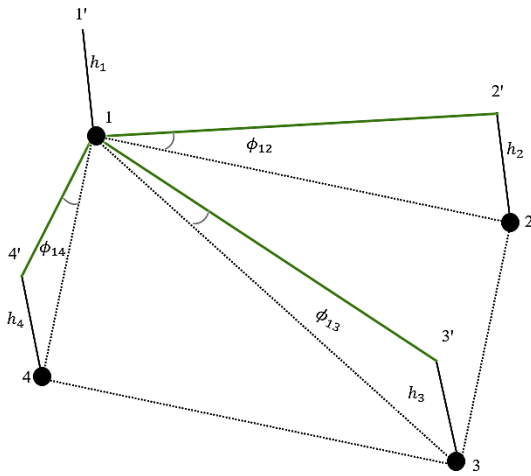


Fig. 1. Bearing elevation angle measurement in 2D

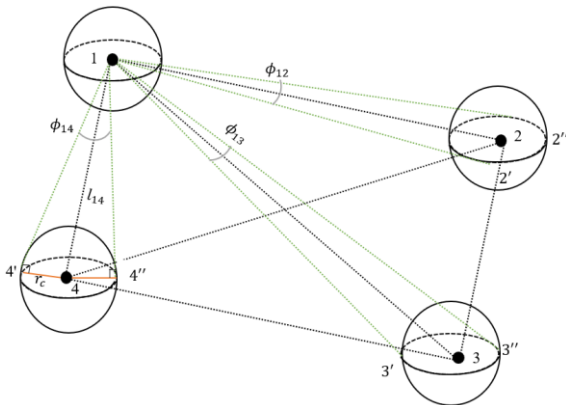


Fig. 2. Bearing elevation angle measurement in 3D

The process of determining an object's position or direction relative to a reference point (node 1) in Fig. 1 is expressed in degrees from true north or magnetic north [84]. In the three-dimensional space of Fig. 2, the elevation angle is used to determine an object's vertical position relative to the reference point. Each node is located at the center of a virtual sphere representing the 3D space with a radius $r_c > 0$. Based on Equation (2), each quadcopter's position (node i) in 3D space can be uniquely identified with no overlapping points $p_i \neq p_j$ for $i \neq j$. The bearing vector b_{ij} is thus obtained as:

$$b_{ij} = \frac{p_j - p_i}{\|p_j - p_i\|} = \frac{p_{ij}}{l_{ij}} \tag{9}$$

where, p_{ij} is the vector from the node i to j , and l_{ij} is the Euclidean distance between i and j . The bearing measurement method serves to maintain specific formations within the quadcopter group. This study assumes equal altitude for all agents relative to the reference point (virtual leader):

$$h_i = h_j = h_c \tag{10}$$

The target formations are fundamental circular and elliptical patterns. This method operates by exploiting geometric relationships between agents, enabling precise coordination among quadcopters. The geometric constraints allow bearing measurement to serve as an effective solution for multi-quadcopter formation control.

D. Flocking Algorithm

The proposed multi-agent system approach focuses on flocking principles in dynamic systems to achieve efficient and adaptive formation for quadcopter groups. The Flocking Algorithm enables the creation of coordinated swarm formations where agents move synchronously despite having only limited knowledge of other agents' positions and states [53]. Based on each agent's dynamic motion (1), with an interaction range $r > 0$ between agents. The quadcopter movement control strategy considers three key parameters:

Separation:

$$f_{sep} = \sum_{j \neq i} \frac{P_i - P_j}{|P_i - P_j|^2} \tag{11}$$

Alignment:

$$f_{align} = \frac{1}{N} \sum_{j \neq i} (v_j - v_i) \tag{12}$$

Cohesion:

$$f_{coh} = \left(\frac{1}{N} \sum_{j \neq i} P_j \right) - P_i \tag{13}$$

A point-set configuration is employed where each point maintains equal distance to all neighboring agents, establishing a lattice structure:

$$\|P_i - P_j\| = d, \quad \forall j \in n_i(P) \tag{14}$$

E. Twisted Sliding Mode Control (TSMC)

This control method guides the system to smoothly reach target states (desired positions), with the "twisted" component reducing chattering effects common in conventional SMC.

The sliding surface design:

$$s = (x - x_{ref}) + \lambda(\dot{x} - \dot{x}_{ref}) \tag{15}$$

where, x is the actual position of the quadcopter, x_{ref} is the reference position and, λ is the control parameter that determines the speed of convergence.

The TSMC sliding surface (s) determines system behavior during sliding mode, ensuring rapid and smooth convergence. TSMC control inputs are given on the Equation (16).

The control law:

$$u_{TSMC} = -k \cdot \text{sign}(s) - \eta \cdot \text{sign}(\dot{s}) \tag{16}$$

Where, k and η are control parameters that determine system response, and $\text{sign}()$ is a signum function. This guarantees both the sliding surface (s) and its derivative (\dot{s}) reach zero. Providing enhanced robustness against disturbances and model uncertainties.

To clarify the workflow and component integration within the system, Fig. 3 presents a flowchart illustrating the key steps in the formation strategy for basic circular and elliptical patterns in multi-quadcopter systems. The following is a flow diagram of the research that has been carried out.

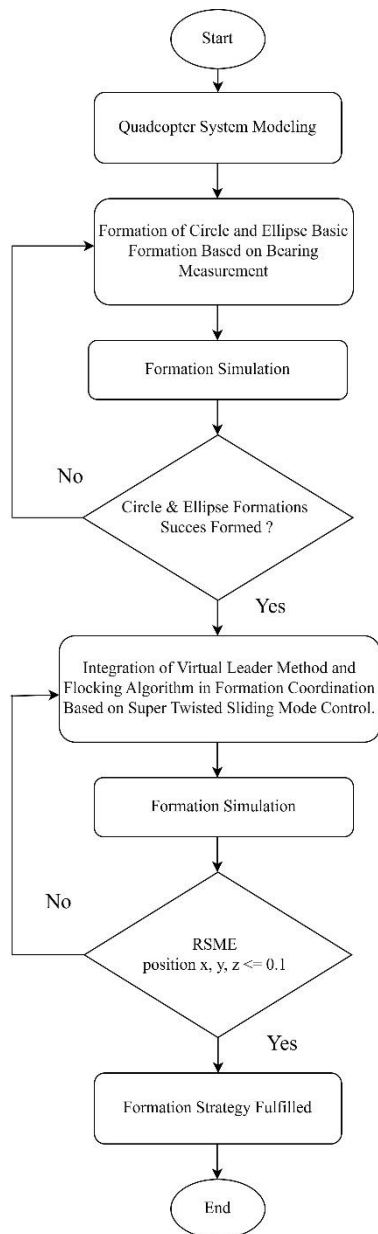


Fig. 3. Research flow diagram

The formation strategy development process for multi-quadcopter systems, as shown in Fig. 3, begins with quadcopter dynamics and kinematics modeling. The quadcopter system model (4) will be used to simulate the formation strategy and formation control system. This research implements circular and elliptical formations using the bearing measurement method. According to Fig. 1, with node 1 as the virtual leader, each quadcopter measures bearing (azimuth and elevation) relative to the virtual leader. A circular formation is achieved when the x and y region coordinates are equal in magnitude, if the size of the x and y regions is different, an elliptical formation will be formed.

The formation is maintained to remain stable and precise when carrying out missions with the flocking algorithm. The principles of separation, alignment, and cohesion (11)-(13) to achieve a coordinated formation. To produce a formation strategy with high precision, TSMC's control system is implemented. The formation strategy will result in stable and coordinated performance.

III. RESULTS AND DISCUSSION

In this section, the results will first show the formation of the basic circle and ellipse shapes based on bearing measurement. Second, the application of the virtual leader and flocking algorithm will be presented once the formation has been successfully established with dynamic movement. Third, the system will be given Twisted Sliding Mode Control to observe the system's stability in maintaining the formation during the assigned mission. The results of the formation of the basic circle and ellipse shapes based on bearing measurement are presented as follows.

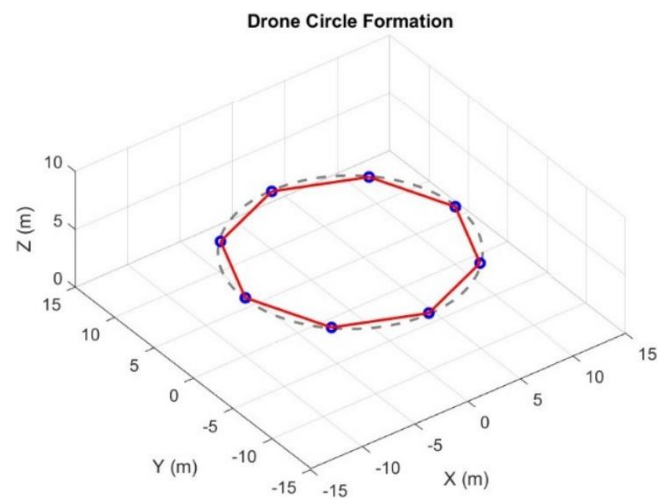


Fig. 4. Circular formation shape results based on bearing measurement

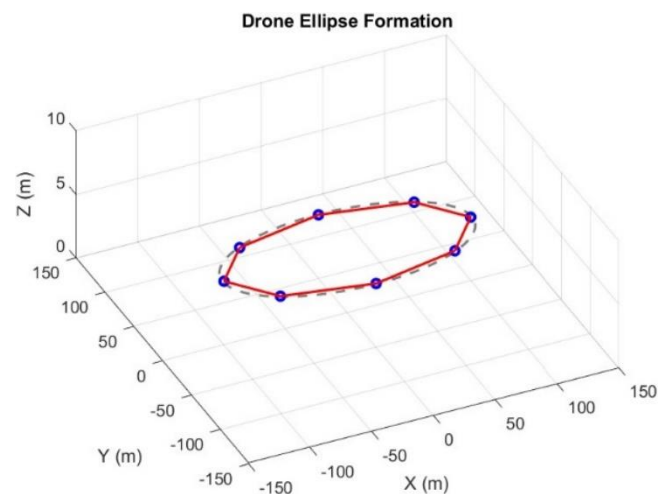


Fig. 5. Elliptical formation shape results based on bearing measurement

Fig. 4 and Fig. 5 show that each agent occupies a position in the circular and elliptical formations with coordinates x, y, and z. The blue dots represent the positions of the quadcopter agents in the circular and elliptical shapes, the red lines connect each agent to form the perimeter of the circle and ellipse, and the dashed lines indicate the ideal reference shapes of the circle and ellipse as formation guidelines. The horizontal angle θ_i (7) is used to ensure that each agent occupies the correct position in the circular and elliptical formations. The bearing measurement algorithm has proven effective in forming circular and elliptical formations, as the coordination between agents functions well, demonstrated by the even distribution of agents along the basic circular and elliptical shapes.

Second, a simulation of the formation of basic circular and elliptical shapes has been conducted, where the formation can move by following a reference point (virtual leader) as a guide for each quadcopter agent. The simulation was performed using Matlab R2022a with 10 active agents. The circular formation was established with a radius of 10 meters, and the minimum distance between agents d_{min} was 0.5 meters. The following are the results of the formation of basic circular and elliptical shapes using the bearing measurement method, integrated with the virtual leader and flocking algorithm.

All agents in Fig. 6 successfully occupy their designated positions, establishing a stable circular formation with uniform distribution. Each agent promptly adjusts its position and velocity in response to real-time positional changes. The vertical coordination is maintained with all agents evenly distributed at 22 meters altitude along the z-axis, ensuring complete formation stability.

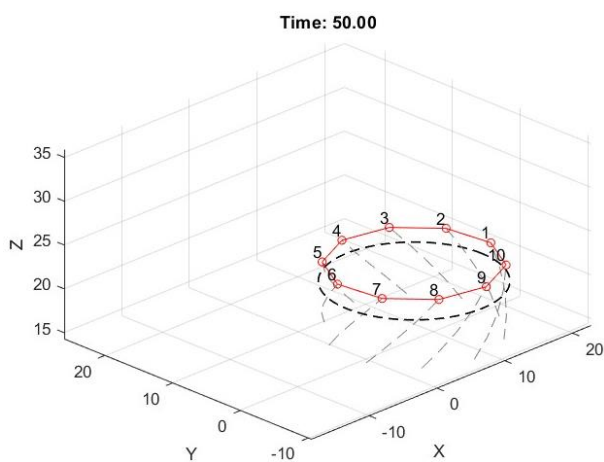


Fig. 6. Circular formation based on virtual leader and flocking

The error data in Table I show that each agent consistently follows the circular reference determined by the virtual leader at the center coordinate (0, 0, 0). A transient phase occurs between seconds 1 to 10, where the error decreases from 0.14 to 0.07 across all axes. A spike in error occurs at t=41 s, but it then stabilizes again, proving that the virtual leader successfully guides the agents to the reference trajectory.

TABLE I. POSITION ERROR IN X, Y, Z FOR DYNAMIC CIRCULAR FORMATION

Time (s)	Error Position X	Error Position Y	Error Position Z
1	0.14	0.14	0.14
10	0.07	0.07	0.07
20	0.07	0.07	0.07
40	0.07	0.07	0.07
41	0.24	0.24	0.24
43	0.06	0.06	0.06
45	0.06	0.06	0.06
47	0.07	0.07	0.07
49	0.08	0.08	0.08
50	0.08	0.08	0.08

The Root Mean Square Error (RMSE) values in Table II represent the average error between the actual agent positions and the target positions. The RMSE values for the x, y, and z positions are all 0.1, indicating that all agents maintain

positions very close to the target formation path. The minimum distance between agents d_{min} is 0.5 m, ensuring that no agent comes closer than this threshold to avoid collisions. Thus, an RMSE position error of 0.1 meters across all axes confirms that the system configuration is safe for each quadcopter agent. The consistent error values across all coordinates reflect the uniformity of the strategy applied in each dimension.

TABLE II. RMSE VALUE OF THE BASE FORMATION POSITION OF THE CIRCLE

Position (m)	x	y	z
RMSE	0.1	0.1	0.1

The performance of the system using the flocking method is capable of maintaining a safe distance between agents (separation), aligning velocities (alignment), and keeping agents within the group (cohesion). Thus, all flocking stages are fulfilled in forming the basic elliptical formation with a minor axis of 100 and a major axis of 50, as shown in Fig. 7. In Table III, the error values for each x, y, and z position achieved in the elliptical formation at an altitude of 22 meters within 50 seconds are obtained.

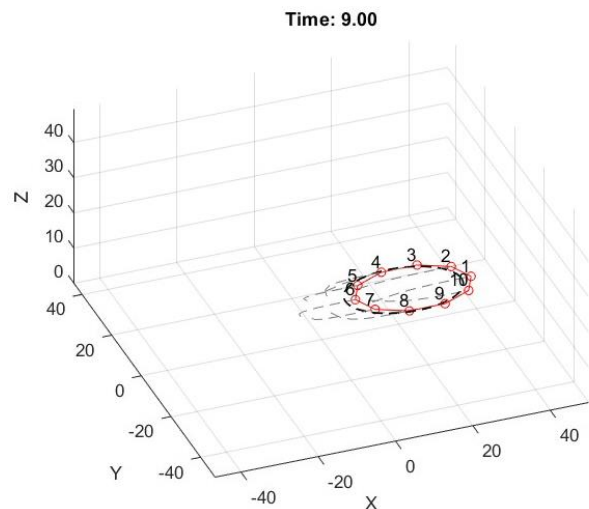


Fig. 7. Elliptical formation based on virtual leader and flocking

TABLE III. POSITION ERROR IN X, Y, Z FOR DYNAMIC ELLIPTICAL FORMATION

Time (s)	Error Position X	Error Position Y	Error Position Z
1	0.17	0.17	0.17
10	0.07	0.07	0.07
20	0.07	0.07	0.07
40	0.07	0.07	0.07
41	0.30	0.30	0.30
43	0.07	0.07	0.07
45	0.07	0.07	0.07
47	0.09	0.09	0.09
49	0.09	0.09	0.09
50	0.09	0.09	0.09

Most of the values in Table III show an error range of 0.07 to 0.09, indicating high precision. In the first second, the error is high due to system adaptation. A spike in error occurs at the 41st second but stabilizes within 2 seconds. This is similar to the performance results in the circular formation, as shown in Table I. The error experiences a significant increase at the

41st second, which may be due to each agent undergoing substantial position changes along the x and y axes. Consequently, the system performs an avoidance maneuver or experiences a sudden setpoint change, leading to a large transient response. Although the z position increases gradually, the drastic changes in x and y positions due to dynamic movement over time cause a response delay. However, rapid recovery, aided by the cohesion and separation rules, helps stabilize the relative position.

The position error values in the x, y, and z coordinates of 0.1 are still within the system's tolerance limit of 0.1 (shown in Table IV). The RMSE in the elliptical formation is the same as in the circular formation, as the elliptical shape has two main parameters, the semi-major and semi-minor axes making agent coordination more complex. Small positioning errors in the elliptical formation tend to accumulate more easily due to the asymmetric distribution of agents compared to the circular formation.

TABLE IV. RMSE VALUE OF THE BASE FORMATION POSITION OF THE ELLIPTICAL

Position (m)	x	y	z
RMSE	0.1	0.1	0.1

Next, the system will be integrated with Twisting Sliding Mode Control (TSMC). In the simulation, the parameters used are $\lambda=2$; $k=0.5$; and $\eta=1.5$, which aim to enhance the agents ability to maintain formation while executing a predefined trajectory mission.

The square trajectory in Fig. 8 is formed by a circular formation consisting of 10 active agents, reaching a maximum altitude of 22 meters within 50 seconds. The circular formation moves dynamically, following a reference

point (virtual leader) located at the center of the circular formation, with a radius of 10 meters. Each agent's position changes over time due to continuous dynamic movement until the square trajectory is fully formed. Below are the x, y, and z positions of each agent over time until reaching an altitude of 22 meters.

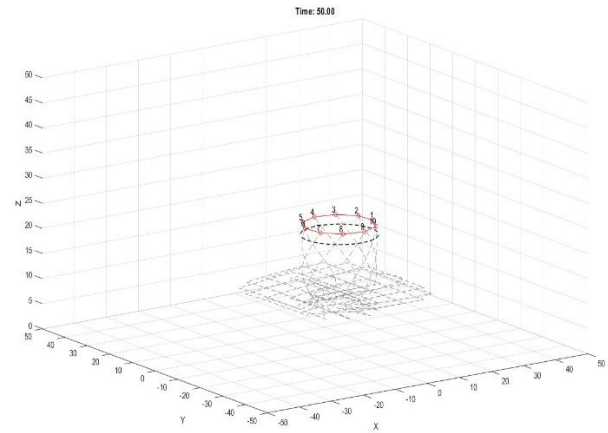


Fig. 8. Circular formation forms a square trajectory

Table V and Table VI present the x and y position data of agents 1 through 10 from the simulation results of forming a square trajectory with a circular formation. The active multi-quadcopter agents complete the mission dynamically by maintaining a circular formation while following the square path. The displayed data is based on changes in altitude (z position) as the system executes the mission. Each agent maintains a uniform altitude of 5 meters from 1 to 40 seconds, corresponding to the phase in which the square trajectory is being formed. From 41 to 50 seconds, the altitude of each agent increases until reaching the predetermined maximum height of 22 meters.

TABLE V. X POSITIONS OF EACH AGENT FORMING A SQUARE TRAJECTORY WITH A CIRCULAR FORMATION

Time	X Position									
	Agent 1	Agent 2	Agent 3	Agent 4	Agent 5	Agent 6	Agent 7	Agent 8	Agent 9	Agent 10
1	12.19	11.69	5.30	6.14	2.24	-1.39	0.47	4.31	9.45	11.99
5	25.99	24.16	19.08	13.34	8.40	6.39	8.29	13.22	19.34	24.18
10	38.73	36.82	31.82	25.65	20.66	18.74	20.65	25.65	31.83	36.82
15	38.74	36.83	31.83	25.65	20.65	18.74	20.65	25.65	31.83	36.83
20	38.74	36.83	31.83	25.65	20.65	18.74	20.65	25.65	31.83	36.83
25	26.24	24.33	19.33	13.15	8.15	6.24	8.15	13.15	19.33	24.33
30	13.74	11.83	6.83	0.65	-4.35	-6.26	-4.35	0.65	6.83	11.83
35	13.74	11.83	6.83	0.65	-4.35	-6.26	-4.35	0.65	6.83	11.83
40	13.74	11.83	6.83	0.65	-4.35	-6.26	-4.35	0.65	6.83	11.83
49	12.56	13.12	10.09	4.63	-1.16	-5.09	-5.64	-2.61	2.84	8.64
50	13.15	12.47	8.46	2.64	-2.76	-5.67	-5.00	-0.98	4.84	10.23

TABLE VI. Y POSITIONS OF EACH AGENT FORMING A SQUARE TRAJECTORY WITH A CIRCULAR FORMATION

Time	Y Position									
	Agent 1	Agent 2	Agent 3	Agent 4	Agent 5	Agent 6	Agent 7	Agent 8	Agent 9	Agent 10
1	4.09	11.09	12.84	10.48	10.24	4.01	2.47	3.12	2.51	5.16
5	6.45	12.39	15.91	15.76	12.34	6.44	0.83	-2.53	-2.57	1.00
10	6.60	12.48	16.11	16.10	12.48	6.60	0.73	-2.90	-2.90	0.73
15	19.10	24.98	28.61	28.61	24.98	19.10	13.22	9.59	9.59	13.22
20	31.60	37.48	41.11	41.11	37.48	31.60	25.72	22.09	22.09	25.72
25	31.60	37.48	41.11	41.11	37.48	31.60	25.72	22.09	22.09	25.72
30	31.60	37.48	41.11	41.11	37.48	31.60	25.72	22.09	22.09	25.72
35	19.10	24.98	28.61	28.61	24.98	19.10	13.22	9.59	9.59	13.22
40	6.60	12.48	16.11	16.11	12.48	6.60	0.72	-2.91	-2.91	0.72
49	2.79	8.71	13.82	16.17	14.87	10.41	4.50	-0.61	-2.97	-1.67
50	4.70	10.59	14.97	16.14	13.68	8.51	2.61	-1.76	-2.94	-0.47

The system achieves a high level of accuracy with an RMSE value of 0.08, as shown in Table VII. Each agent successfully maintains a 10-meter distance from the virtual leader using bearing measurement. The inter-agent distance remains under 0.5 meters due to the implementation of the flocking lattice algorithm. Next, a simulation of an elliptical formation was conducted with the mission of forming a square trajectory.

TABLE VII. RMSE VALUES OF POSITION FOR EACH AGENT FORMING A SQUARE TRAJECTORY WITH A CIRCULAR FORMATION

Position (m)	x	y	z
RMSE	0.08	0.08	0.08

The results in Fig. 9 show that the elliptical formation dynamically follows a square trajectory. The elliptical formation consists of 10 active agents. The x, y, and z positions of each agent change over time as they navigate the trajectory. Below is the position data for each agent in the elliptical formation, illustrating their movement throughout the mission.

The position data of each active agent in Tables VIII and IX are the results of the simulation forming a square trajectory with an elliptical formation, as shown in Fig. 9. The x and y positions change dynamically over time to complete the square trajectory mission. The altitude of each active agent remains the same, as it follows the altitude of the reference point (virtual leader). Below are the RMSE values for each agent's position in the elliptical formation during the square trajectory mission.

The RMSE values for all positions x, y, and z in the elliptical formation are the same at 0.09 (shown in Table X). This error is higher than in the circular formation due to the varying curvature in the dynamically formed ellipse, which requires continuous adjustments in bearing measurement and inter-agent distance, increasing the risk of collision or separation loss. Additionally, non-uniform velocity changes in the elliptical formation, particularly along the minor and major axes, contribute to this increase in error. However, the RMSE reduction of 0.01 to 0.02 in the circular formation indicates improved precision, primarily due to the influence of the integrated TSMC control. Dynamic stability is well maintained during trajectory transitions.

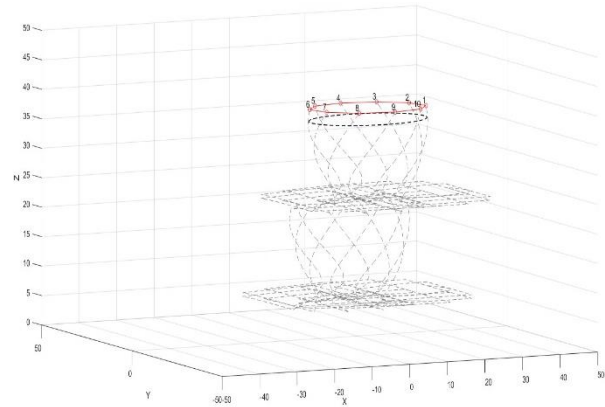


Fig. 9. Elliptical formation forms a square trajectory

TABLE VIII. X POSITIONS OF EACH AGENT FORMING A SQUARE TRAJECTORY WITH A ELLIPTICAL FORMATION

X Position										
Time	Agent 1	Agent 2	Agent 3	Agent 4	Agent 5	Agent 6	Agent 7	Agent 8	Agent 9	Agent 10
1	14.69	13.72	6.07	5.37	0.21	-3.89	-1.56	3.54	10.22	14.01
5	30.83	28.08	20.57	11.84	4.49	1.54	4.37	11.72	20.83	28.10
10	43.73	40.86	33.36	24.11	16.62	13.75	16.61	24.11	33.37	40.87
15	43.74	40.87	33.37	24.10	16.60	13.74	16.60	24.10	33.37	40.87
20	43.74	40.87	33.37	24.10	16.60	13.74	16.60	24.10	33.37	40.87
25	31.24	28.37	20.87	11.60	4.10	1.24	4.10	11.60	20.87	28.37
30	18.74	15.87	8.37	-0.90	-8.40	-11.26	-8.40	-0.90	8.37	15.87
35	18.74	15.87	8.37	-0.90	-8.40	-11.26	-8.40	-0.90	8.37	15.87
40	18.74	15.87	8.37	-0.90	-8.40	-11.26	-8.40	-0.90	8.37	15.87
49	16.98	16.69	11.45	3.27	-4.73	-9.50	-9.21	-3.98	4.21	12.21
50	17.86	16.28	9.91	1.19	-6.56	-10.38	-8.80	-2.44	6.29	14.04

TABLE IX. Y POSITIONS OF EACH AGENT FORMING A SQUARE TRAJECTORY WITH A ELLIPTICAL FORMATION

Y Position										
Time	Agent 1	Agent 2	Agent 3	Agent 4	Agent 5	Agent 6	Agent 7	Agent 8	Agent 9	Agent 10
1	4.09	11.09	12.84	10.48	10.24	4.01	2.47	3.12	2.51	5.16
5	6.45	12.39	15.91	15.76	12.34	6.44	0.83	-2.53	-2.57	1.00
10	6.60	12.48	16.11	16.10	12.48	6.60	0.73	-2.90	-2.90	0.73
15	19.10	24.98	28.61	28.61	24.98	19.10	13.22	9.59	9.59	13.22
20	31.60	37.48	41.11	41.11	37.48	31.60	25.72	22.09	22.09	25.72
25	31.60	37.48	41.11	41.11	37.48	31.60	25.72	22.09	22.09	25.72
30	31.60	37.48	41.11	41.11	37.48	31.60	25.72	22.09	22.09	25.72
35	19.10	24.98	28.61	28.61	24.98	19.10	13.22	9.59	9.59	13.22
40	6.60	12.48	16.11	16.11	12.48	6.60	0.72	-2.91	-2.91	0.72
49	0.89	7.17	13.23	16.76	16.41	12.32	6.04	-0.03	-3.56	-3.21
50	3.74	9.82	14.67	16.44	14.45	9.46	3.38	-1.47	-3.23	-1.24

TABLE X. RMSE VALUES OF POSITION FOR EACH AGENT FORMING A SQUARE TRAJECTORY WITH A ELLIPTICAL FORMATION

Position (m)	x	y	z
RMSE	0.09	0.09	0.09

IV. CONCLUSION

The formation of basic circular and elliptical shapes is achieved with high accuracy using the bearing measurement method and flocking algorithm based on a virtual leader. This is evidenced by the RMSE values for both circular and elliptical formations, which are 0.1 across all three position coordinates (x, y, and z). The designed system effectively maintains formation accuracy for both circular and elliptical geometries, demonstrating consistent performance across different shapes. The addition of TSMC control significantly enhances stability and ensures that each agent remains robustly within the formation. The square trajectory was successfully formed with consistently low RMSE values of 0.08 and 0.09. Further research is needed to implement a more robust control system to minimize errors and enhance system stability. The current study has been conducted in a MATLAB simulation environment. Future research will focus on simulations in real-world environments or Software-in-the-Loop (SITL). Additionally, the research can be extended to experimental validation using quadcopter hardware.

ACKNOWLEDGMENT

The authors express their sincere gratitude to Institut Teknologi Sepuluh Nopember, the Department of Engineering Physics (No: 741/IT.2.I.2/T/HK.00.02/XI/2024), the Instrumentation, Control, and Optimization Laboratory, as well as the Embedded Systems and Cyber-Physical Systems Laboratory.

REFERENCES

- [1] P. Y. Leong and N. S. Ahmad, "Exploring Autonomous Load-Carrying Mobile Robots in Indoor Settings: A Comprehensive Review," *IEEE Access*, vol. 12, pp. 131395–131417, 2024, doi: 10.1109/ACCESS.2024.3435689.
- [2] W. Malik and S. Hussain, "Developing of the smart quadcopter with improved flight dynamics and stability," *J. Electr. Syst. Inf. Technol.*, vol. 6, no. 1, pp. 1–8, 2019, doi: 10.1186/s43067-019-0005-0.
- [3] L. A. Fagundes, J. Kevin, B. D. C. Ricardo, and S. F. Alexandre, "Machine Learning for Unmanned Aerial Vehicles Navigation: An Overview," *SN Comput. Sci.*, 2024, doi: 10.1007/s42979-023-02592-5.
- [4] B. Mishra, D. Garg, P. Narang, and V. Mishra, "Drone-surveillance for search and rescue in natural disaster," *Comput. Commun.*, vol. 156, pp. 1–10, 2020, doi: 10.1016/j.comcom.2020.03.012.
- [5] A. Albanese, V. Sciancalepore, and X. Costa-Perez, "SARDO: An Automated Search-and-Rescue Drone-Based Solution for Victims Localization," *IEEE Trans. Mob. Comput.*, vol. 21, no. 9, pp. 3312–3325, 2022, doi: 10.1109/TMC.2021.3051273.
- [6] M. H. Rahman, M. A. S. Sejan, M. A. Aziz, R. Tabassum, J. I. Baik, and H. K. Song, "A Comprehensive Survey of Unmanned Aerial Vehicles Detection and Classification Using Machine Learning Approach: Challenges, Solutions, and Future Directions," *Remote Sens.*, vol. 16, no. 5, 2024, doi: 10.3390/rs16050879.
- [7] S. A. H. Mohsan, N. Q. H. Othman, Y. Li, M. H. Alsharif, and M. A. Khan, "Unmanned aerial vehicles (UAVs): practical aspects, applications, open challenges, security issues, and future trends," *Intell. Serv. Robot.*, vol. 16, no. 1, pp. 109–137, 2023, doi: 10.1007/s11370-022-00452-4.
- [8] J. Yousaf *et al.*, "Drone and Controller Detection and Localization: Trends and Challenges," *Appl. Sci.*, vol. 12, no. 24, 2022, doi: 10.3390/app122412612.
- [9] K. Kim, "User Preferences in Drone Design and Operation," *Drones*, vol. 6, no. 5, 2022, doi: 10.3390/drones6050133.
- [10] K. Telli *et al.*, "A Comprehensive Review of Recent Research Trends on Unmanned Aerial Vehicles (UAVs)," *Systems*, vol. 11, no. 8, pp. 1–48, 2023, doi: 10.3390/systems11080400.
- [11] Z. Zhang, X. Xu, J. Cui, and W. Meng, "Multi-uav area coverage based on relative localization: Algorithms and optimal uav placement," *Sensors*, vol. 21, no. 7, pp. 1–14, 2021, doi: 10.3390/s21072400.
- [12] S. M. S. Mohd Daud *et al.*, "Applications of drone in disaster management: A scoping review," *Sci. Justice*, vol. 62, no. 1, pp. 30–42, 2022, doi: 10.1016/j.scijus.2021.11.002.
- [13] N. Jia, Z. Yang, and K. Yang, "Operational effectiveness evaluation of the swarming UAVs combat system based on a system dynamics model," *IEEE Access*, vol. 7, pp. 25209–25224, 2019, doi: 10.1109/ACCESS.2019.2898728.
- [14] J. Gui, T. Yu, B. Deng, X. Zhu, and W. Yao, "Decentralized Multi-UAV Cooperative Exploration Using Dynamic Centroid-Based Area Partition," *Drones*, vol. 7, no. 6, pp. 1–15, 2023, doi: 10.3390/drones7060337.
- [15] X. An, C. Wu, Y. Lin, M. Lin, T. Yoshinaga, and Y. Ji, "Multi-Robot Systems and Cooperative Object Transport: Communications, Platforms, and Challenges," *IEEE Open J. Comput. Soc.*, vol. 4, 2022, pp. 23–36, 2023, doi: 10.1109/OJCS.2023.3238324.
- [16] V. G. Nair, J. M. D'souza, and K. R. Guruprasad, "Optimizing Multi-Agent Search with Non-Uniform Sensor Effectiveness in Distributed Quadcopter Systems," *IEEE Access*, vol. 12, pp. 85531–85550, 2024, doi: 10.1109/ACCESS.2024.3413596.
- [17] K. S. Bin Gaufan, S. El-Ferik, and N. M. Alyazidi, "Fractional Model-Based Formation Control of Quad-Rotor UAVs Using Sliding Mode Backstepping," *IEEE Access*, vol. 12, 2024, doi: 10.1109/ACCESS.2024.3489630.
- [18] M. A. Al-Absi, A. A. Al-Absi, M. Sain, and H. Lee, "Moving ad hoc networks—a comparative study," *Sustain.*, vol. 13, no. 11, 2021, doi: 10.3390/su13116187.
- [19] M. A. Luna, M. Molina, R. Da-Silva-Gomez, J. Melero-Deza, P. Arias-Perez, and P. Campoy, "A multi-UAV system for coverage path planning applications with in-flight re-planning capabilities," *J. F. Robot.*, 2024, doi: 10.1002/rob.22342.
- [20] L. Chen and Z. Wang, "Multi-UAV trajectory planning for RIS-assisted SWIPT system under connectivity preservation," *Comput. Networks*, vol. 255, p. 110906, 2024, doi: 10.1016/j.comnet.2024.110906.
- [21] J. P. Queralt *et al.*, "Collaborative multi-robot search and rescue: Planning, coordination, perception, and active vision," *IEEE Access*, vol. 8, pp. 191617–191643, 2020, doi: 10.1109/ACCESS.2020.3030190.
- [22] H. A. Hung, H. H. Hsu, and T. H. Cheng, "Optimal Sensing for Tracking Task by Heterogeneous Multi-UAV Systems," *IEEE Trans. Control Syst. Technol.*, vol. 32, no. 1, pp. 282–289, 2024, doi: 10.1109/TCST.2023.3298487.
- [23] J. Wang, K. Li, and K. Xia, "Distributed formation control of multi-UAV systems using relative information," *J. Franklin Inst.*, vol. 361, no. 10, p. 106945, 2024, doi: 10.1016/j.jfranklin.2024.106945.
- [24] X. Dong, Y. Hua, Y. Zhou, Z. Ren, and Y. Zhong, "Theory and Experiment on Formation-Containment Control of Multiple Multirotor Unmanned Aerial Vehicle Systems," *IEEE Trans. Autom. Sci. Eng.*, vol. 16, no. 1, pp. 229–240, 2019, doi: 10.1109/TASE.2018.2792327.
- [25] J. Alonso-Mora, E. Montijano, T. Nageli, O. Hilliges, M. Schwager, and D. Rus, "Distributed multi-robot formation control in dynamic environments," *Auton. Robots*, vol. 43, no. 5, pp. 1079–1100, 2019, doi: 10.1007/s10514-018-9783-9.
- [26] W. Pang, D. Zhu, and C. Sun, "Multi-AUV Formation Reconfiguration Obstacle Avoidance Algorithm Based on Affine Transformation and Improved Artificial Potential Field under Ocean Currents Disturbance," *IEEE Trans. Autom. Sci. Eng.*, vol. 21, no. 2, pp. 1469–1487, 2024, doi: 10.1109/TASE.2023.3245818.
- [27] L. Bian, W. Sun, and T. Sun, "Trajectory following and Improved Differential Evolution Solution for Rapid Forming of UAV Formation," *IEEE Access*, vol. 7, pp. 169599–169613, 2019, doi: 10.1109/ACCESS.2019.2954408.

- [28] Q. Feng *et al.*, "Resilience Measure and Formation Reconfiguration Optimization for Multi-UAV Systems," *IEEE Internet Things J.*, vol. 11, no. 6, pp. 10616–10626, 2024, doi: 10.1109/IIOT.2023.3326552.
- [29] S. Naderi and M. J. Blondin, "A Mapping and State-of-the-Art Survey on Multi-Objective Optimization Methods for Multi-Agent Systems," *IEEE Access*, vol. 11, pp. 139728–139744, 2023, doi: 10.1109/ACCESS.2023.3341295.
- [30] M. Doostmohammadian, A. Taghieh, and H. Zarrabi, "Distributed Estimation Approach for Tracking a Mobile Target via Formation of UAVs," *IEEE Trans. Autom. Sci. Eng.*, vol. 19, no. 4, pp. 3765–3776, 2022, doi: 10.1109/TASE.2021.3135834.
- [31] B. Li *et al.*, "Multi-UAV Trajectory Planning during Cooperative Tracking Based on a Fusion Algorithm Integrating MPC and Standoff," *Drones*, vol. 7, no. 3, 2023, doi: 10.3390/drones7030196.
- [32] C. Tao, R. Zhang, Z. Song, B. Wang, and Y. Jin, "Multi-UAV Formation Control in Complex Conditions Based on Improved Consistency Algorithm," *Drones*, vol. 7, no. 3, 2023, doi: 10.3390/drones7030185.
- [33] L. F. C. Ccari and P. R. Yanyachi, "A Novel Neural Network-Based Robust Adaptive Formation Control for Cooperative Transport of a Payload Using Two Underactuated Quadcopters," *IEEE Access*, vol. 11, pp. 36015–36028, 2023, doi: 10.1109/ACCESS.2023.3265957.
- [34] J. Choi, Y. Song, S. Lim, C. Kwon, and H. Oh, "Decentralized multi-subgroup formation control with connectivity preservation and collision avoidance," *IEEE Access*, vol. 8, pp. 71525–71534, 2020, doi: 10.1109/ACCESS.2020.2987348.
- [35] N. P. Nguyen *et al.*, "Quadrotor Formation Control via Terminal Sliding Mode Approach: Theory and Experiment Results," *Drones*, vol. 6, no. 7, 2022, doi: 10.3390/drones6070172.
- [36] M. B. Sial *et al.*, "Bearing-Based Distributed Formation Control of Unmanned Aerial Vehicle Swarm by Quaternion-Based Attitude Synchronization in Three-Dimensional Space," *Drones*, vol. 6, no. 9, 2022, doi: 10.3390/drones6090227.
- [37] L. Zhao, Y. Liu, Q. Peng, and L. Zhao, "A Dual Aircraft Maneuver Formation Controller for MAV/UAV Based on the Hybrid Intelligent Agent," *Drones*, vol. 7, no. 5, 2023, doi: 10.3390/drones7050282.
- [38] Z. G. Xiong, Y. S. Luo, Z. Liu, and Z. K. Liu, "Suboptimal Relational Tree Configuration and Robust Control Based on the Leader-follower Model for Self-organizing Systems Without GPS Support," *Int. J. Control. Autom. Syst.*, vol. 22, no. 4, pp. 1442–1454, 2024, doi: 10.1007/s12555-022-0505-x.
- [39] L. Smolentsev, A. Krupa, and F. Chaumette, "Shape Visual Servoing of A Cable Suspended Between Two Drones," *IEEE Robot. Autom. Lett.*, vol. 9, no. 12, pp. 11473–11480, 2024, doi: 10.1109/LRA.2024.3494655.
- [40] X. Cai, X. Zhu, and W. Yao, "Distributed time-varying out formation-containment tracking of multi-UAV systems based on finite-time event-triggered control," *Sci. Rep.*, vol. 12, no. 1, pp. 1–16, 2022, doi: 10.1038/s41598-022-24083-y.
- [41] I. H. Imran, D. F. Kurtulus, A. M. Memon, S. Goli, T. Kouser, and L. M. Alhems, "Distributed Robust Formation Control of Heterogeneous Multi-UAVs With Disturbance Rejection," *IEEE Access*, vol. 12, pp. 55326–55341, 2024, doi: 10.1109/ACCESS.2024.3390183.
- [42] R. Li, Y. Tang, and S. Li, "Robust Positive Consensus for Heterogeneous Multi-agent Systems," *Int. J. Control. Autom. Syst.*, vol. 22, no. 4, pp. 1129–1137, 2024, doi: 10.1007/s12555-022-1201-6.
- [43] X. Gao, C. Chen, and Z. Xiang, "Consensus for Nonlinear Multiagent Systems via Hybrid Event-Triggered Mechanism," *IEEE Syst. J.*, vol. 18, no. 4, pp. 2022–2029, 2024, doi: 10.1109/JSYST.2024.3488968.
- [44] T. Kwak, Y. Kim, Y. Hori, and T. H. Kim, "Graphical and Analytical Approaches for Analyzing Collective Behavior of Dynamic Multi-Agent Systems Governed by Generalized Cyclic Pursuit Mechanism," *IEEE Access*, vol. 11, pp. 140481–140495, 2023, doi: 10.1109/ACCESS.2023.3339195.
- [45] Z. Pan, C. Zhang, Y. Xia, H. Xiong, and X. Shao, "An Improved Artificial Potential Field Method for Path Planning and Formation Control of the Multi-UAV Systems," *IEEE Trans. Circuits Syst. II Express Briefs*, vol. 69, no. 3, pp. 1129–1133, 2022, doi: 10.1109/TCSII.2021.3112787.
- [46] Y. Tang, H. Chen, Z. Ma, Z. Jin, and H. Yin, "Application of Artificial Potential Field Method in Three-Dimensional Path Planning for UAV Considering 5G Communication," *IEEE Access*, vol. 12, pp. 79238–79250, 2024, doi: 10.1109/ACCESS.2024.3406560.
- [47] L. Zhai, C. Liu, X. Zhang, and C. Wang, "Local Trajectory Planning for Obstacle Avoidance of Unmanned Tracked Vehicles Based on Artificial Potential Field Method," *IEEE Access*, vol. 12, pp. 19665–19681, 2024, doi: 10.1109/ACCESS.2024.3355952.
- [48] J. Sun, J. Tang, and S. Lao, "Collision Avoidance for Cooperative UAVs with Optimized Artificial Potential Field Algorithm," *IEEE Access*, vol. 5, pp. 18382–18390, 2017, doi: 10.1109/ACCESS.2017.2746752.
- [49] K. K. Oh, M. C. Park, and H. S. Ahn, "A survey of multi-agent formation control," *Automatica*, vol. 53, pp. 424–440, 2015, doi: 10.1016/j.automatica.2014.10.022.
- [50] A. Singha, A. K. Ray, and A. B. Samaddar, "Leader-Follower Based Formation Controller Design for Quadrotor UAVs," *Trans. Indian Natl. Acad. Eng.*, vol. 7, no. 1, pp. 325–338, 2022, doi: 10.1007/s41403-021-00305-z.
- [51] C. Ren, F. Fu, C. Yin, Z. Yan, R. Zhang, and Z. Wang, "Improved artificial potential field method based on robot local path information," *Int. J. Adv. Robot. Syst.*, vol. 21, no. 5, pp. 1–16, 2024, doi: 10.1177/17298806241278172.
- [52] J. Yan, Y. Yu, Y. Xu, and X. Wang, "A Virtual Point-Oriented Control for Distance-Based Directed Formation and Its Application to Small Fixed-Wing UAVs," *Drones*, vol. 6, no. 10, 2022, doi: 10.3390/drones6100298.
- [53] R. Olfati-Saber, "Flocking for multi-agent dynamic systems: Algorithms and theory," *IEEE Trans. Automat. Contr.*, vol. 51, no. 3, pp. 401–420, 2006, doi: 10.1109/TAC.2005.864190.
- [54] C. Song, L. Liu, and S. Xu, "Circle formation control of mobile agents with limited interaction range," *IEEE Trans. Automat. Contr.*, vol. 64, no. 5, pp. 2115–2121, 2019, doi: 10.1109/TAC.2018.2866985.
- [55] S. M. M. S. Sajadi and H. Atrianfar, "Dynamic Circular Formation Of Multi-Agent Systems With Obstacle Avoidance And Size Scaling: A Flocking Approach," *arXiv preprint arXiv:2212.12554*, 2022.
- [56] S. Kim, H. Cho, and D. Jung, "Circular Formation Guidance of Fixed-Wing UAVs Using Mesh Network," *IEEE Access*, vol. 10, pp. 115295–115306, 2022, doi: 10.1109/ACCESS.2022.3218673.
- [57] H. Su, S. Zhu, C. Chen, Z. Yang, and X. Guan, "Bearing-Based Robust Formation Tracking Control of Underactuated AUVs with Optimal Parameter Tuning," *IEEE Trans. Cybern.*, vol. 54, no. 7, pp. 4049–4062, 2024, doi: 10.1109/TCYB.2023.3346654.
- [58] Y. Li, P. Zhang, Z. Wang, D. Rong, M. Niu, and C. Liu, "Multi-UAV Obstacle Avoidance and Formation Control in Unknown Environments," *Drones*, vol. 8, no. 12, 2024, doi: 10.3390/drones8120714.
- [59] P. Zhang, Z. Wang, Z. Zhu, Q. Liang, and J. Luo, *Enhanced Multi-UAV Formation Control and Obstacle Avoidance Using IAAPF-SMC*, vol. 8, no. 9, 2024, doi: 10.3390/drones8090514.
- [60] H. Li, J. Hu, Q. Zhou, and B. K. Ghosh, "Safe formation control of multiple unmanned aerial vehicles: control design and safety-stability analysis," *Control Theory Technol.*, vol. 22, no. 3, pp. 442–454, 2024, doi: 10.1007/s11768-024-00209-7.
- [61] Y. Liu, Z. Liu, G. Wang, C. Yan, X. Wang, and Z. Huang, "Flexible multi-UAV formation control via integrating deep reinforcement learning and affine transformations," *Aerosp. Sci. Technol.*, vol. 157, p. 109812, 2025, doi: 10.1016/j.ast.2024.109812.
- [62] C. Bao, Y. Guo, L. Luo, and G. Su, "Design of a Fixed-Wing UAV Controller Based on Adaptive Backstepping Sliding Mode Control Method," *IEEE Access*, vol. 9, pp. 157825–157841, 2021, doi: 10.1109/ACCESS.2021.3130296.
- [63] N. P. Agustina and P. A. Darwito, "Autonomous Quadcopter Trajectory Tracking and Stabilization Using Control System Based on Sliding Mode Control and Kalman Filter," *2023 Int. Semin. Intell. Technol. Its Appl.*, pp. 489–493, 2023, doi: 10.1109/ISITIA59021.2023.10221176.
- [64] C. Kuchwa-Dube and J. O. Pedro, "Chattering performance criteria for multi-objective optimisation gain tuning of sliding mode controllers," *Control Eng. Pract.*, vol. 127, p. 105284, 2022, doi: 10.1016/j.conengprac.2022.105284.
- [65] Y. B. Shtessel, J. A. Moreno, and L. M. Fridman, "Twisting sliding mode control with adaptation: Lyapunov design, methodology and

- application,” *Automatica*, vol. 75, pp. 229–235, 2017, doi: 10.1016/j.automatica.2016.09.004.
- [66] B. Li, X. Gao, H. Huang, and H. Yang, “Improved adaptive twisting sliding mode control for trajectory tracking of an AUV subject to uncertainties,” *Ocean Eng.*, vol. 297, p. 116204, 2024, doi: 10.1016/j.oceaneng.2023.116204.
- [67] B. Yan, P. Dai, R. Liu, M. Xing, and S. Liu, “Adaptive super-twisting sliding mode control of variable sweep morphing aircraft,” *Aerosp. Sci. Technol.*, vol. 92, pp. 198–210, 2019, doi: 10.1016/j.ast.2019.05.063.
- [68] H. Tiaiba, M. E. H. Daachi, and T. Madani, “Real-time adaptive super twisting algorithm based on PSO algorithm: Application for an exoskeleton robot,” *Robotica*, vol. 42, no. 6, pp. 1816–1841, 2024, doi: 10.1017/S0263574724000547.
- [69] A. Nandanwar *et al.*, “Stochastic Event-Based Super-Twisting Formation Control for Multiagent System Under Network Uncertainties,” *IEEE Trans. Control Netw. Syst.*, vol. 9, no. 2, pp. 966–978, 2022, doi: 10.1109/TCNS.2021.3089142.
- [70] H. Gao, W. Li, and H. Cai, “Fully Distributed Robust Formation Flying Control of Drones Swarm Based on Minimal Virtual Leader Information,” *Drones*, vol. 6, no. 10, 2022, doi: 10.3390/drones6100266.
- [71] B. Yildiz, M. F. Aslan, A. Durdu, and A. Kayabasi, “Consensus-based virtual leader tracking swarm algorithm with GDRRT*-PSO for path-planning of multiple-UAVs,” *Swarm Evol. Comput.*, vol. 88, p. 101612, 2024, doi: 10.1016/j.swevo.2024.101612.
- [72] J. A. Vazquez Trejo *et al.*, “Robust Formation Control Based on Leader-Following Consensus in Multi-Agent Systems with Faults in the Information Exchange: Application in a Fleet of Unmanned Aerial Vehicles,” *IEEE Access*, vol. 9, pp. 104940–104949, 2021, doi: 10.1109/ACCESS.2021.3098303.
- [73] A. Ebrahimi and M. Farrokhi, “Multi-agent flocking with obstacle avoidance and safety distance preservation: a fuzzy potential-based approach,” *Intell. Serv. Robot.*, vol. 17, no. 2, pp. 181–195, 2024, doi: 10.1007/s11370-023-00500-7.
- [74] J. Wu, Y. Ji, X. Sun, and W. Liang, “Virtual-leader Split/Rejoin-based Flocking Control With Obstacle Avoidance for Multi-agents,” *Int. J. Control. Autom. Syst.*, vol. 22, no. 5, pp. 1680–1690, 2024, doi: 10.1007/s12555-022-0950-6.
- [75] V. Utkin, A. Poznyak, Y. Orlov, and A. Polyakov, “Conventional and high order sliding mode control,” *J. Franklin Inst.*, vol. 357, no. 15, pp. 10244–10261, 2020, doi: 10.1016/j.jfranklin.2020.06.018.
- [76] Z. Wang and Y. Luo, “Elliptical Multi-Orbit Circumnavigation Control of UAVS in Three-Dimensional Space Depending on Angle Information Only,” *Drones*, vol. 6, no. 10, 2022, doi: 10.3390/drones6100296.
- [77] Q. Wu, Y. Zeng, and R. Zhang, “Joint Trajectory and Communication Design for Multi-UAV Enabled Wireless Networks,” *IEEE Trans. Wirel. Commun.*, vol. 17, no. 3, pp. 2109–2121, 2018, doi: 10.1109/TWC.2017.2789293.
- [78] F. Zitouni, S. Harous, and R. Maamri, “A Distributed Approach to the Multi-Robot Task Allocation Problem Using the Consensus-Based Bundle Algorithm and Ant Colony System,” in *IEEE Access*, vol. 8, pp. 27479–27494, 2020, doi: 10.1109/ACCESS.2020.2971585.
- [79] H. Li, H. Li, X. Li, and X. Li, “Distributed consensus of heterogeneous linear time-varying systems on UAVs-USVs coordination,” *IEEE Trans. Circuits Syst. II Express Briefs*, vol. 67, no. 7, pp. 1264–1268, 2020, doi: 10.1109/TCSII.2019.2928870.
- [80] N. P. Agustina, “Control System on Multi-Quadcopter Based Sliding Mode Control (SMC) - Extended Kalman Filter (EKF) to Generate Optimal Trajectory Tracking Stability,” *2024 Int. Conf. Smart Comput. IoT Mach. Learn.*, pp. 19–24, 2024, doi: 10.1109/SIML61815.2024.10578288.
- [81] Z. Wang, Y. Zou, Y. Liu, and Z. Meng, “Distributed Control Algorithm for Leader-Follower Formation Tracking of Multiple Quadrotors: Theory and Experiment,” in *IEEE/ASME Transactions on Mechatronics*, vol. 26, no. 2, pp. 1095–1105, April 2021, doi: 10.1109/TMECH.2020.3017816.
- [82] B. Measurements *et al.*, “Adaptive Formation Tracking Control of Multiple Vertical Takeoff and Landing UAVs With,” *IEEE Trans. Cybern.*, vol. 54, no. 6, pp. 3491–3501, 2024, doi: 10.1109/TCYB.2023.3290726.
- [83] M. Ye, B. D. O. Anderson, and C. Yu, “Bearing-Only Measurement Self-Localization , Velocity Consensus and Formation Control,” *IEEE Trans. Aerosp. Electron. Syst.*, vol. 53, no. 2, pp. 575–586, 2017, doi: 10.1109/TAES.2017.2651538.
- [84] L. Chen and Z. Sun, “Gradient-based bearing-only formation control: An elevation angle approach,” *Automatica*, vol. 141, p. 110310, 2022, doi: 10.1016/j.automatica.2022.110310.